J Mater Sci (2016) 51:5625–5634

Controlled thermal functionalization for dispersion enhancement of multi-wall carbon nanotube in organic solvents

Xuelong Chen[1], Xiu-Zhi Tang[1], Yen Nan Liang[1], Jun Wei Cheah[1], Peng Hu[1], and Xiao Hu[1,*]

[1] *School of Material Science and Engineering, Nanyang Technological University, Nanyang Avenue, Singapore 639798, Singapore*

Received: 13 December 2015
Accepted: 27 February 2016
Published online: 8 March 2016

ABSTRACT

Despite extensive study on carbon nanotube (CNT), the proliferation of its real applications has been hindered by its dispersibility in various organic or inorganic media. Very often complex surface functionalization processes are required to endow CNTs with enhanced dispersibility. Hence, facile, high-yield, and scalable functionalization methods for CNT for better dispersion are highly desirable. Thermal annealing is sometimes adopted for purification of CNT; however, limited discussion has been devoted to its functionalization effect and surface chemistry, which directly determine CNT dispersibility. In this work, via controlled mild thermal annealing, enhanced dispersion of functionalized CNTs was achieved in different organic solvents, including ethanol, dimethyl formamide, chloroform and acetone. Such enhancement had been studied through qualitative (dispersion and sedimentation, TEM) and quantitative analyses (XPS, Raman) of morphological structures and chemical states of thermally functionalized CNTs. The analyses reveal that under mild thermal annealing conditions, the surface oxidative reactions of the CNT can be well controlled, with minimal damage to the graphitic structure of the CNT. A plausible functionalization mechanism involving ether and quinone functional groups is proposed. The advantages of thermal annealing toward enhanced dispersion are further demonstrated by employing the functionalized CNT in poly (vinylidene fluoride) composite and drop-cast conductive CNT pattern.

Introduction

In the past two decades, carbon nanotubes (CNTs) as a quasi-1D material have been extensively investigated because of their unique and outstanding mechanical, chemical, electrical, electronic, and thermal properties. Their applications include, but not limited to, composite materials, sensors, photovoltaic devices, actuators, transistors, and energy storage devices [1–3]. However, due to the typical high aspect ratio (>100) and existing Van der Waals forces

Address correspondence to E-mail: ASXHU@ntu.edu.sg

DOI 10.1007/s10853-016-9864-0

between CNTs, they usually form highly entangled bundles [4]. Such entanglement of CNTs causes poor dispersion in any solvent and seriously hinders their potential applications. Multiple strategies have been explored to disperse CNTs in various solvents via covalent and non-covalent modifications. Oxidation by strong acids is often a common and effective chemical modification, which introduces polar surface functional groups, e.g. carboxylic, hydroxyl, and ketone groups, to render good dispersion in mainly aqueous medium [5, 6]. Despite the effectiveness of acid/chemical oxidation, the drawbacks of this approach are obvious. Its required usage of large quantity of strong acids limits industrial scale production and causes pollution. Another method is non-covalent physical wrapping of polymers on the surface of CNTs, which can also improve CNT dispersion [7, 8]. Unlike oxidation, physical wrapping does not directly introduce new functional groups on CNTs. The polymer chains usually interact physically with CNTs to form a supramolecular structure. However, these physically wrapping polymers have to be specially designed and involve tedious synthesis steps, again limiting its practicality.

Thermal annealing is widely adopted to process carbon materials, contributed by its simplicity, scalability, and environmental friendliness [9, 10]. It is known that annealing at high temperature in inert atmosphere generates more graphitic CNTs by removing dangling bonds and functional groups, while annealing at low temperature in oxidative gas (e.g. air or ozone) could have multiple effects on CNTs structures [11, 12]. Yang et al. functionalized MWCNTs in air at 500 °C and demonstrated enhanced catalytic performance for wet air oxidation of phenol contributed by introduced oxygen-containing functional groups [13]. Li et al. [14] and Seo et al. [15] reported improved electric double layer capacitance of MWCNTs thermally annealed in air, contributed by the increased surface area. Kung et al. [16] and Zeng et al. [17] studied the effects of heat treatment in air toward field emission of MWCNTs. They found lowered onset emission voltage and enhanced emission current with thermal annealing, which was claimed to be the result of selectively opened CNTs tips and increased surface area. We would like to highlight that most of the previous works on thermal annealing of CNTs focused on CNT-based device performance, paying little attention to relationship between surface chemistry during thermal functionalization, as well as the dispersion behaviour in organic solvents. In this work, by controlling the thermal annealing conditions, we studied the effects of relatively mild annealing in oxidative atmosphere toward MWCNTs dispersion. Under the controlled conditions, the structural integrity of the CNT was maintained during our mild thermal annealing, at the same time promising high functionalized CNT yield. We propose a new mechanism that involves the formation of oxygen-containing surface ether C–O–C and quinone C=O functional groups, which directly help enhancing the CNT dispersion.

Experimental section

Materials

Multi-wall carbon nanotubes (MWCNTs) with average diameter of 10 nm and average length of 1.5 μm were purchased from Nanocyl, Belgium. The surface area of CNTs is 250–300 m^2/g. Poly (vinylidene fluoride) (PVDF) powder was purchased from Alfa Aesar. The solvents used, which include analytical grade ethanol, acetone, chloroform and N, N-Dimethylformamide (DMF), were purchased from Sigma Aldrich.

Thermal annealing

Annealing process was performed using a Thermal Gravimetric Analyser (Q 500, TA Instruments). Raw CNTs without any pre-treatment were placed in a platinum boat and were heated up in air with a flow rate of 5 mL/min, to the pre-set temperature between 350 and 550 °C at 5 °C/min.

Characterizations

The morphology of CNTs was studied using transmission electron microscope (TEM) (Carl Zeiss Libra 120 Plus). The fractural morphology of prepared composite samples was studied by field emission scanning electron microscope (FESEM) (JEOL JSM-7600F). SEM samples were prepared by firstly immersing the CNT/polymer composites inside liquid nitrogen before fracturing them, and then the fractural surfaces were coated with platinum for 45 s before SEM observation. Compositional analysis of CNTs was carried out using an X-ray photoelectron

spectroscopy (XPS) equipped with an Axis Ultra spectrometer (Kratos Analytical). A monochromatic Al Kα X-ray (1486.7 eV) operating at 15 kV was used as the source. Raman spectra were recorded by a Witec Alpha 300 SR spectrometer with an Argon ion laser (488 nm, 20mW) as the excitation source. For each sample, five Raman spectra were recorded at difference sample locations. To test the electrical resistivity of thermally annealed CNTs, 0.5 mg CNTs were dispersed in 10 mL ethanol and drop cast at 50 °C on glass with patterned ITO electrodes. The electrical measurement was done by Hewlett Packard 4140B pA Meter/DC Voltage source. The *I–V* curves were measured over a range of 0.2 to −0.2 V, with a step of 0.01 V in normal ambient.

Results and discussion

One of the main objectives of this work is to effectively functionalize CNTs in oxidative atmosphere at elevated temperature, at the same time not damaging their structural integrity to ensure highest possible functionalized CNT yield. Therefore, a minimal air flow rate i.e. 5 mL/min was employed in this study. The annealing temperature range was decided to be between 350 and 550 °C. In fact, oxidation only occurs above a critical temperature and accelerates as temperature increases; too high the temperature leads to rapid and excessive oxidation of CNTs, resulting in low yields. For example, our separate work showed that heating CNTs up to 650 °C led to 59 % weight loss. Although the thermally annealed CNTs can form stable solvent dispersion for months, observation of morphologies using TEM revealed substantial damage of the graphitic structure (Figure S1), which compromises its electrical properties.

Figure 1a shows the weight loss of various thermally treated samples. At 350 °C, the residue mass is almost constant from 30 to 120 min of annealing duration, suggesting that CNTs are insensitive to oxidation at this temperature. Higher annealing temperature expectedly leads to higher oxidation rate. For heating above 400 °C, the weight loss increases with longer annealing duration. When treated at 450 °C for 30 min (A3), 96.4 wt% CNTs were obtained. With prolonged annealing duration to 60 (B3), 90 (C3) and 120 min (D3), the residue mass decreased to 95.8, 93.8 and 91.9 %, respectively. At fixed 60-min annealing duration, the residue mass for samples treated at 400, 450, 500 and 550 °C are 98.0, 95.8, 74.1 and 34.7 wt%, respectively. The oxidation is greatly accelerated at 90 min@550 °C annealing and almost no carbon-based material remained, leaving behind only metal oxide catalytic materials (C5 and D5).

With successful thermal functionalization, the introduced oxygen-containing groups on CNTs are able to form hydrogen bonding with polar solvents (e.g. ethanol) leading to enhanced dispersibility of CNTs. However, samples annealed at 350 °C with different durations (A1, B1, C1 and D1) were poorly dispersed (Fig. 1b), indicating ineffective functionalization. Minimal weight loss and no clear improvement of dispersibility were observed for the samples

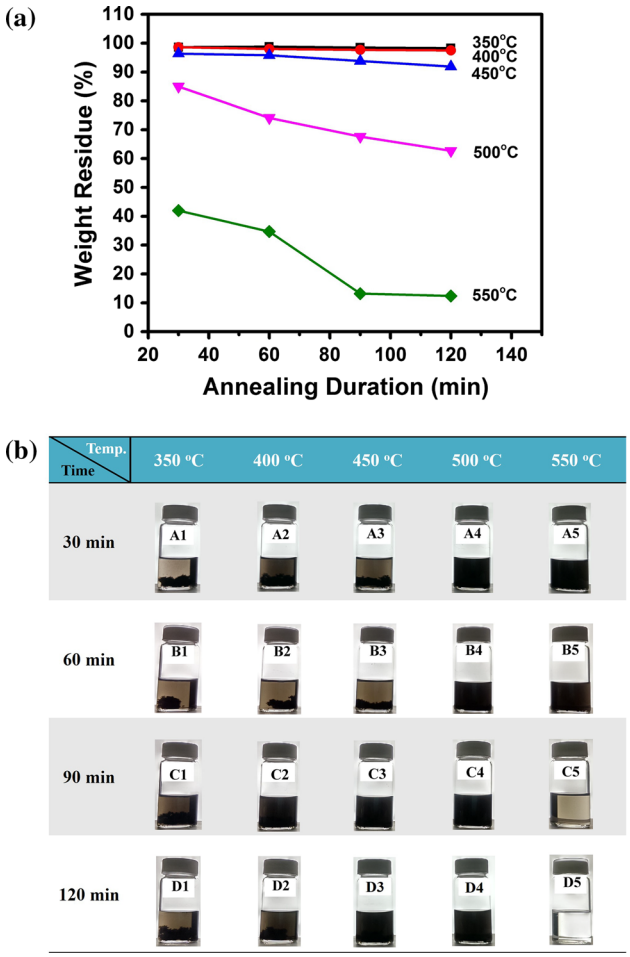

Figure 1 The residue masses at different annealing conditions (**a**) and digital photographs of 1-week CNTs dispersion samples, prepared by sonicating 0.5 mg CNTs in 10 mL ethanol for 60 min (**b**). Labelled on glass vials are the sample codes corresponding to different thermal functionalization conditions.

annealed at 400 °C from 30 to 120 min (A2, B2, C2 and D2). Samples annealed at 450 °C with shorter duration (A3: 30 min and B3: 60 min) also could not be dispersed well in ethanol. Nevertheless, the fact that better dispersibility of CNTs followed by extended annealing duration (C3, 90 min and D3, 120 min) suggested that certain amount of oxygen-containing groups had formed on CNTs at 450 °C. All four samples annealed at 500 °C (A4, B4, C4 and D4) showed satisfactory dispersibility in ethanol. High enough annealed CNT yields were also achieved under this temperature, i.e. 85.0, 74.1, 67.6 and 62.7 wt% respectively for annealing duration from 30 to 120 min. The yield is much higher than that of similar previous work that employed air as to purify CNTs, which is believed to be contributed by much milder oxidation with minimal air flow rate in this study [18]. Higher annealing temperature at 550 °C is much more effective in oxidizing CNTs. Samples treated at this temperature with short duration of 30 or 60 min (A5 and B5) showed very good dispersibility. However, the annealing yield is low, which were 42.0 and 34.7 wt%. The structural integrity of CNTs annealed under these conditions had been compromised. Longer annealing durations (C5: 90 min and D5: 120 min) led to formation of metal oxide residue, which is impossible to be dispersed in ethanol. Besides ethanol, representative organic solvents with different polarities, i.e. acetone, chloroform and DMF were also found to be able to disperse well the thermally functionalized CNTs (Figure S2).

From the dispersion test, annealed samples A4 (30 min@500 °C) and D3 (120 min@450 °C) showed that their conditions are optimal, contributed by the combined high yields and excellent dispersibility of CNTs. To examine their surface morphologies, TEM (shown in Fig. 2) was employed. Comparing with that of raw CNTs, it can be seen that samples A4 and D3 have similar overall morphology with subtly rougher surfaces (Fig. 2b, c inset images). The defects and particles generated on the CNTs surface evidenced the successful functionalization via thermal annealing. The weight losses for both samples are less than 15 %, mainly attributed to the evaporation of moisture and elimination of amorphous carbon, while not including the oxidative gasification of carbon atoms. These results again demonstrate that controlled thermal annealing can facilely functionalize CNT at high yield and achieve excellent dispersion in organic solvents, without excessively

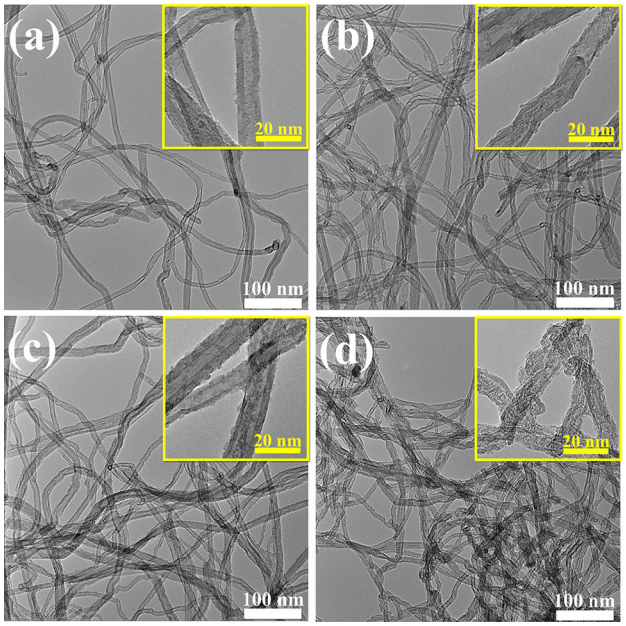

Figure 2 TEM images of **a** raw CNTs and annealed CNTs under different conditions: **b** A4, 30 min@500 °C **c** D3, 120 min@450 °C and **d** B5, 60 min@550 °C. The *insets* are enlarged images showing structural changes after thermal functionalization; in which CNT surface of sample A4 and D3 is well preserved while that of B5 is clearly damaged.

damaging the integrity of the graphitic structure. Conventional CNT functionalization by boiling acids severely damages the graphitic structure of the CNTs, creating a relatively thick amorphous layer on outer surface of CNTs [19]. Such amorphous layer adversely affects the thermal stability and electrical properties. Obvious structural damage because of the rapid and excess oxidation at this temperature could be observed in sample B5 (Fig. 2d). It is well accepted that the CNT tips, as well as bends and kinks within the tubular structures, bear more strain and are more prone to be attacked upon oxidation. Thus, CNT surfaces are likely to be opened or cut at these positions, leading to shorter tubes with varied curvatures [20]. No obvious CNTs fragmentation effect or curvature changes were observed from our TEM images, which are believed to be caused by the mild oxidative condition used in this work. Nevertheless, the CNT surface of sample B5 is thinner than that of raw CNTs, indicating that the outer layers of CNTs have been 'etched off' via oxidation.

The effect of thermal functionalization toward the surface chemistry of CNT was further investigated by Raman spectroscopy. It is well known that Raman effect is sensitive to any chemical modifications of

CNT, such as any introduced defects and new functional groups [14, 21, 22]. Raman spectra were collected from groups with fixed annealing duration (A1, A2, A3, A4 and A5) and temperature (A3, B3, C3 and D3), as shown in Fig. 3. The peak called D band around 1350 cm^{-1}, representing sp^3 carbon atoms, is closely related to the integrity and intactness of the graphitic structure. The intensity of D band increases with the increase of defects sites, impurities, and the amount of amorphous carbon [23]. The peak at 1570 cm^{-1} is called G band, which comes from the conjugated carbon atoms of sp^2 hybridization. The I_D/I_G intensity ratio is a frequently used indicator of defects on CNTs. When temperature increased from 350 to 450 °C, I_D/I_G values of A1, A2 and A3 also increased slightly, indicating very minor oxidation. It is known that thermal annealing has dual effects toward CNTs structure. On one hand, CNT can be oxidized and new defects sites formed, contributing to the D band. On the other hand, amorphous carbon on the CNT surface can be effectively eliminated, reducing the intensity of D band. It is believed that the amorphous carbon was largely reduced in A4 sample, which effects overwhelmed that of the newly formed defects, leading to an eventual suppressed I_D/I_G value. Similar phenomenon was also reported by other group [18]. The large increase of I_D/I_G value from A4 to A5 is caused by the extensive oxidation that created plenty of dangling oxygen-containing groups. Same trend was also observed when CNTs were annealed at fixed temperature and varied durations. Slight increase of I_D/I_G value was observed for A3 and B3 samples, as compared with that of raw CNTs. The I_D/I_G value declined firstly before increasing again, indicating simultaneous elimination of amorphous carbon and creation of new functional groups.

XPS is a useful tool to study the elemental compositions and functional groups on CNTs, either qualitatively or quantitatively [24–27]. Figure 4a shows the C1s and O1s XPS spectra of raw CNTs and representative annealed samples. The oxygen content found in raw CNTs is believed to be due to impurities or catalyst residues. The oxygen content increases after thermal annealing; explaining the enhanced dispersibility of CNTs in organic solvents as more hydrogen bonding is formed. The total oxygen contents of a series of selected samples are summarized in Table 1. The oxygen contents are 5.56, 7.37, 7.42 and 12.93 % for samples A3, A4, D3 and A5,

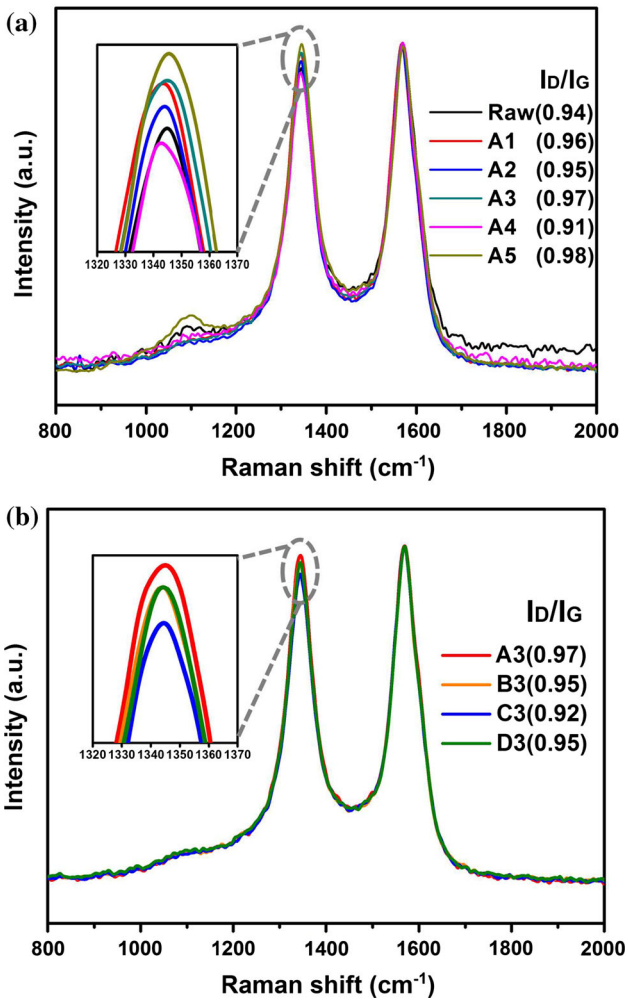

Figure 3 Raman spectra of raw CNTs and annealed samples. **a** CNTs are annealed for 30 min at different temperatures, **b** CNTs are annealed at 450 °C for different durations. The curves are normalized with the G band as the reference, so the I_D/I_G values can be easily compared. The I_D/I_G values of each samples are included inside the *right-hand-side* brackets.

respectively, showing a gradual increasing trend at higher temperature/longer duration.

The deconvoluted C1s and O1s spectra are shown in Fig. 4b–d. The C1s peak for raw CNTs and annealed CNTs can be deconvoluted into and fitted by two sub-peaks. The major peak with a binding energy at 284.8 eV corresponds to sp^2 hybridized carbon atoms of the graphitic structure in the CNTs, while the minor peak at 285.8 eV is assigned to sp^3 hybridized carbon atoms bonded to oxygen [28]. The sp^2 hybridized carbon contents are calculated to be 84.71 82.52, 81.41, 80.25, 76.25 % for of raw CNTs and annealed samples A3, D3, A4 and A5, respectively (Table 1). There is only a small reduction of sp^2

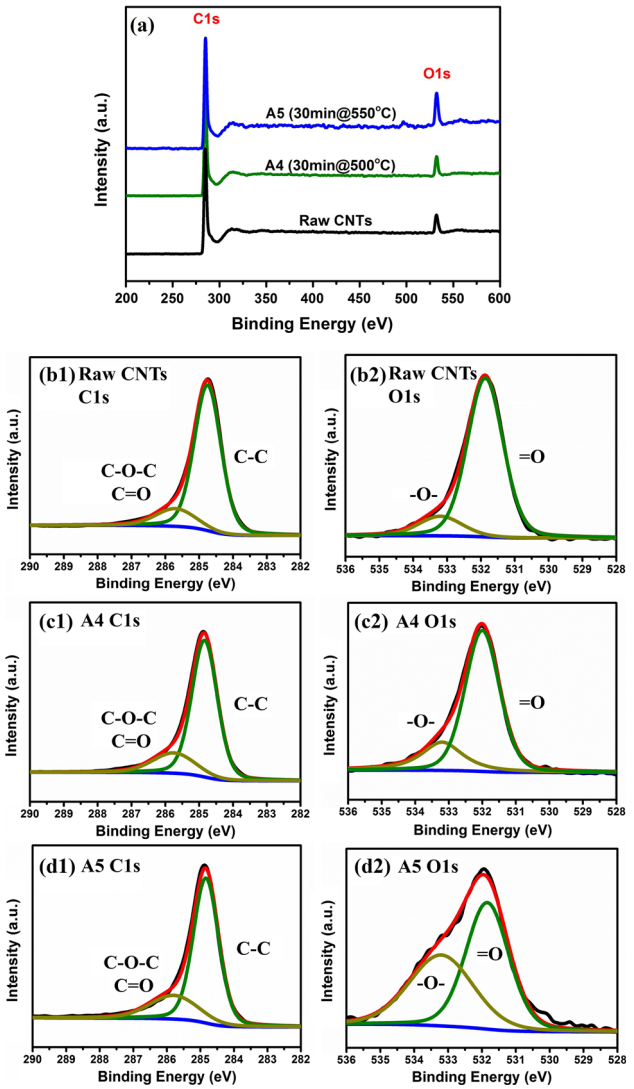

Figure 4 XPS spectra of raw CNTs, sample A4 (30 min@500 °C) and A5 (30 min@550 °C) (**a**) and deconvoluted high resolution XPS C1s spectra of raw CNTs (**b1**) A4 (**c1**) and A5 (**d1**); the corresponding O1s are given in (**b2**), (**c2**) and (**d2**), respectively. The oxygen contents for raw CNTs, A4 and A5 are calculated to be 5.53, 7.37 and 12.93 %, respectively.

carbon content in the annealed samples. Correspondingly, the O1s spectra can also be fitted into two peaks. The lower binding energy peak at 531.9 eV is assigned to be quinone groups (C=O), and the other peak at 533.2 eV belongs to ether groups (C–O–C) [29, 30]. Closer examination of the functional group ratios summarized in Table 1 further reveals that increasing annealing temperature has larger influence on contents of C–O–C and C=O functional groups than that of increasing annealing duration (C1s Table 1). Data derived from O1s spectra in Table 1 show that the relative contents of –O– (related to C–O–C) and =O (related to C=O) are very different when annealed at 450, 500, and 550 °C. It is important to note that higher annealing temperature has clearly favoured the formation of ether groups (C–O–C) at the expense of quinone groups (C=O). For example, the C–O–C group percentage of sample A3 annealed at 450 °C is 16.40 %. It increased to 23.13 and 45.27 % in samples A4 and A5, which were annealed at 500 and 550 °C. It is also noted that samples A4 (30 min@500 °C) and D3 (120 min@450 °C) have almost the same total oxygen content, i.e. 7.37 and 7.42 %. However, the C–O–C to C=O ratio in sample A4 is 0.30 while that in D3 is 0.23. These observations indicate that shorter duration/higher temperature annealing leads to more C–O–C groups than longer duration/lower temperature annealing, while the latter yields more C=O groups. Different from thermal annealing, oxidizing CNTs in strong acids leads to other types of functional groups. Apart from the main peak of graphitic sp^2 around 284.8 eV, acid-treated CNTs also comprise C–OH and COOH [24, 31], which are absent in our thermal-annealed samples. The absence of these two functional groups is an important reason that thermally annealed CNTs has poorer dispersion in aqueous medium, despite well dispersed in organic solvents.

Based on Raman and XPS analyses, we hereby propose a plausible reaction mechanism that involves the formation of surface ether and quinone groups on CNTs during thermal annealing, which are illustrated in Fig. 5. To form C–O–C group, the first and also the determining step is the 1, 4 peroxidation. After that, the π electrons in the two adjacent C=C bonds rearrange and simultaneously form single bonds with the two oxygen atoms, while the –O–O– bond breaks homolytically. On the other hand, the formation of C=O groups begins with a 1, 2 peroxidation on the graphitic ring, and this is followed by simultaneous homolytic breaking of C–C and O–O bond, leading to the formation of two quinone groups. It is seen in XPS analysis that lower temperature is less favourable in generating C–O–C groups, i.e. less favourable to 1, 4 peroxidation. This is reasonable as the activation energy for 1, 4 peroxidation in the planar graphitic ring is higher than that of 1, 2 peroxidation.

Enhanced dispersion of CNTs in organic solvents directly indicates the potential of readily incorporating the thermally functionalized CNTs into polymer

Table 1 Percentages of different C and O oxidation states as determined from XPS spectra

Sample	C 1s		O 1s		Total O wt%
	284.8 eV (C–C) (%)	285.8 eV (C–O–C, C=O) (%)	531.9 eV (=O) (%)	533.2 eV (–O–) (%)	
Raw CNTs	84.71	15.29	84.71	15.29	5.53
A3 (30 min@450 °C)	82.52	17.48	83.60	16.40	5.56
A4 (30 min@500 °C)	80.25	19.75	76.87	23.13	7.37
A5 (30 min@550 °C)	76.25	23.75	54.73	45.27	12.93
D3 (120 min@450 °C)	81.41	18.59	81.37	18.63	7.42

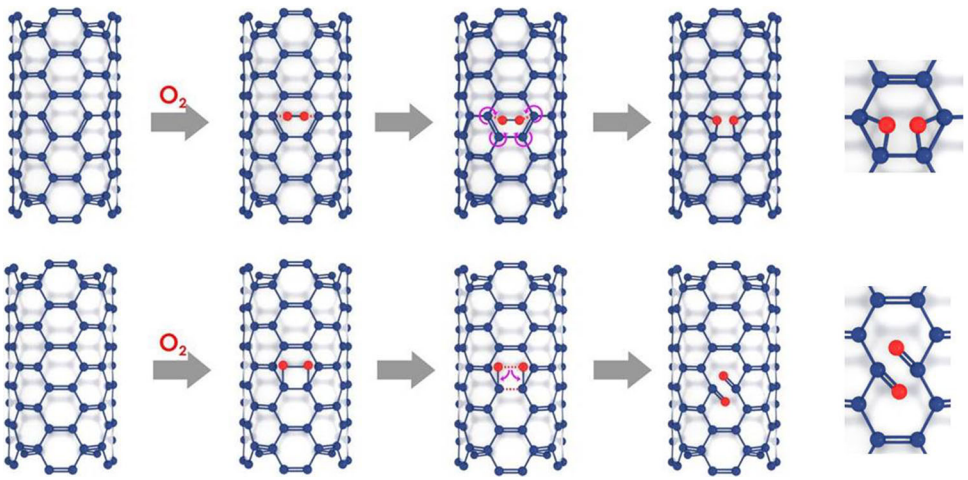

Figure 5 The proposed mechanisms of CNT surface functionalization via thermal annealing. The top part shows the formation of ether functional group, while the bottom part shows the formation of quinone group.

matrices using conventional solution blending approach. To demonstrate such application, we compared composites with annealed CNTs and the raw CNTs dispersed in a PVDF matrix. Figure 6 compares the morphologies of the cryo-fractured morphologies of PVDF composites containing annealed CNT sample (sample D3) and raw CNTs (both 0.2 wt%), prepared by using DMF as the solvent. It can be seen that raw CNTs formed distinct and large aggregations in the polymer matrix (Fig. 7a, b), while annealed CNTs of sample D3 were individually separated and well dispersed throughout the polymer matrix (Fig. 7c, d). Achieving such a good dispersibility of CNTs in a polymer matrix is non-trivial and often requires lengthy and laborious treatment procedures that have poor scalability such as specialized grafting [32, 33].

Good CNTs dispersion, with minimal structural damage, is particularly important for the applications of CNTs as conductive coating or circuitry. Inkjet printing represents one patterning technique that has been employed to fabricate conductive CNT films [34–36]. Despite the efforts, the difficulty to prepare uniformly dispersed CNT printing solution hinders this application. Previous works mostly used acid treated CNTs or surfactant to improve dispersion; however, these methods suffer from process complexity and compromise of electrical conductivity. To demonstrate the feasibility of using thermally functionalized CNTs as printing ink, ethanoic solutions containing annealed CNTs were drop-cast onto ITO patterned glasses, and electrical conductivity was tested. The resistivity of 10 μL of annealed CNTs at 30 min@ 500 °C and raw CNTs without any treatment on ITO patterned glass are shown in Fig. 7. As shown also in the top-left inset are the optical images of samples with different ink volumes. It clearly shows that raw CNTs aggregated after the evaporation of solvent, and they stayed electrically insulated from each other on the ITO patterned glasses, due to the poor dispersion of raw CNTs and poor wetting to the substrate. The conductivity test shows that the

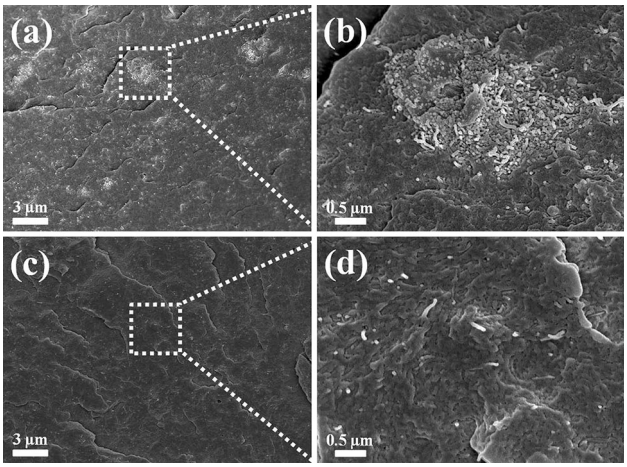

Figure 6 FESEM images showing the cryo-fractured morphologies of PVDF/CNTs composites with 0.2 wt% (**a**, **b**) raw CNT and (**c**, **d**) annealed sample D3.

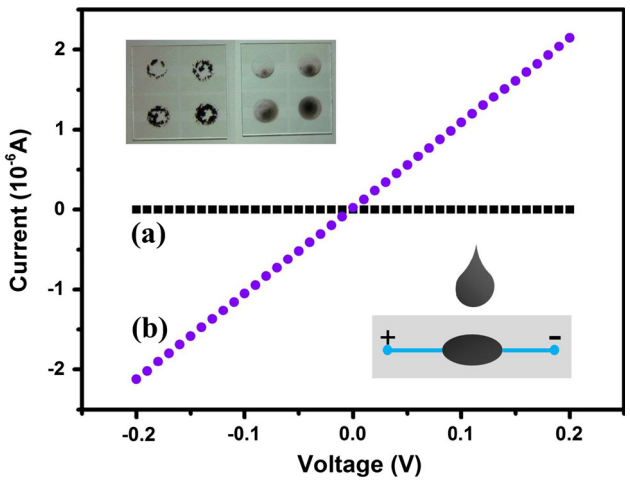

Figure 7 *I–V* curve of drop-cast raw CNTs and thermally functionalized CNTs (A4, 30 min@ 500 °C) on ITO patterned glass. The drop volume is 10 μL. *Top-left inset* shows raw CNTs (*left*) and air-annealed CNTs (*right*) with different volumes (10, 20, 30 and 50 μL) drop-cast on ITO patterned glass. *Bottom right inset* shows the schematic of electrical testing of drop-cast CNTs pattern.

pattern formed by raw CNTs is insulating until the feeding volume increased to 30 μL. By contrast, the thermally functionalized CNTs exhibited good pattern uniformity and obvious electrical conductivity, contributed by the oxygen-containing groups introduced during thermal annealing that enabled the good dispersion of CNTs in organic solvents and enhanced wetting to substrate. Again, it is shown that mild thermal annealing of CNT ensures the elimination of amorphous carbon, introducing functional groups and intactness of graphitic structures, which are critical in ensuring the high conductivity.

Conclusion

In this work, controlled mild thermal functionalization of CNTs was carried out and shown to be an effective route for surface modification of CNTs. This is a facile method which leads to high yield of annealed CNTs as high as 90 %. After annealing at optimal temperature and duration, enhanced dispersion was demonstrated for the annealed CNTs in various organic solvents including ethanol, dimethyl formamide, chloroform and acetone. It was also shown that the controlled thermal annealing caused minimal damage to the graphitic structures of CNTs, as concluded from both Raman and TEM analysis. A plausible functionalization mechanism related to surface chemistry is hereby proposed based on detailed Raman and XPS spectroscopic analyses, i.e. thermal annealing introduced uniform surface ether C–O–C and quinone C=O groups on CNT surface. We further demonstrated that thermal annealing is scalable and the resultant CNTs can be readily used for preparing CNT/polymer composite and fabricating printed electronics. This facile and scalable treatment process for CNTs opens up a lot of opportunities of wide range of applications that requires uniformly dispersion CNTs within an organic media.

Acknowledgements

Xuelong Chen acknowledges the scholarship from Nanyang Technological University. The authors thank the facility for analysis, characterization, testing and simulation (FACTS) lab where material characterizations were performed. This work is also partially supported by A-Star through the MIMO programme.

Electronic supplementary material: The online version of this article (doi:10.1007/s10853-016-9864-0) contains supplementary material, which is available to authorized users.

References

[1] Baughman RH, Zakhidov AA, de Heer WA (2002) Carbon nanotubes—the route toward applications. Science 297(5582): 787–792

[2] Bachtold A, Hadley P, Nakanishi T, Dekker C (2001) Logic circuits with carbon nanotube transistors. Science 294(5545): 1317–1320

[3] Ren S, Bernardi M, Lunt RR, Bulovic V, Grossman JC, Gradecak S (2011) Toward efficient carbon nanotube/p3ht solar cells: active layer morphology, electrical, and optical properties. Nano Lett 11(12):5316–5321

[4] Qin S, Qin D, Ford WT, Herrera JE, Resasco DE, Bachilo SM, Weisman RB (2004) Solubilization and purification of single-wall carbon nanotubes in water by in situ radical polymerization of sodium 4-styrenesulfonate. Macromolecules 37(11):3965–3967

[5] Spitalsky Z, Tasis D, Papagelis K, Galiotis C (2010) Carbon nanotube–polymer composites: chemistry, processing, mechanical and electrical properties. Prog Polym Sci 35(3):357–401

[6] Mazov I, Kuznetsov VL, Simonova IA, Stadnichenko AI, Ishchenko AV, Romanenko AI, Tkachev EN, Anikeeva OB (2012) Oxidation behavior of multiwall carbon nanotubes with different diameters and morphology. Appl Surf Sci 258(17):6272–6280

[7] Chen J, Liu H, Weimer WA, Halls MD, Waldeck DH, Walker GC (2002) Noncovalent engineering of carbon nanotube surfaces by rigid, functional conjugated polymers. J Am Chem Soc 124(31):9034–9035

[8] Star A, Stoddart JF, Steuerman D, Diehl M, Boukai A, Wong EW, Yang X, Chung SW, Choi H, Heath JR (2001) Preparation and properties of polymer-wrapped single-walled carbon nanotubes. Angew Chem Int Ed 40(9):1721–1725

[9] Bhushan B (2010) Springer handbook of nanotechnology. Springer, New York

[10] Klein KL, Melechko AV, McKnight TE, Retterer ST, Rack PD, Fowlkes JD, Joy DC, Simpson ML (2008) Surface characterization and functionalization of carbon nanofibers. J Appl Phys 103(6):061301

[11] Behler K, Osswald S, Ye H, Dimovski S, Gogotsi Y (2006) Effect of thermal treatment on the structure of multi-walled carbon nanotubes. J Nanopart Res 8(5):615–625

[12] Lau CH, Cervini R, Clarke SR, Markovic MG, Matisons JG, Hawkins SC, Huynh CP, Simon GP (2008) The effect of functionalization on structure and electrical conductivity of multi-walled carbon nanotubes. J Nanopart Res 10(1):77–88

[13] Yang S, Wang X, Yang H, Sun Y, Liu Y (2012) Influence of the different oxidation treatment on the performance of multi-walled carbon nanotubes in the catalytic wet air oxidation of phenol. J Hazard Mater 233:18–24

[14] Li C, Wang D, Liang T, Wang X, Wu J, Hu X, Liang J (2004) Oxidation of multiwalled carbon nanotubes by air: benefits for electric double layer capacitors. Powder Technol 142(2):175–179

[15] Seo M-K, Park S-J (2010) Influence of air-oxidation on electric double layer capacitances of multi-walled carbon nanotube electrodes. Curr Appl Phys 10(1):241–244

[16] Kung S-C, Hwang KC, Lin IN (2002) Oxygen and ozone oxidation-enhanced field emission of carbon nanotubes. Appl Phys Lett 80(25):4819–4821

[17] Zeng B, Xiong G, Chen S, Wang W, Wang D, Ren Z (2006) Enhancement of field emission of aligned carbon nanotubes by thermal oxidation. Appl Phys Lett 89(22):223119

[18] Mercier G, Jrm Gleize, Ghanbaja J, Marêché J-F, Vigolo B (2013) Soft oxidation of single-walled carbon nanotube samples. J Phys Chem C 117(16):8522–8529

[19] Shin Y-R, Jeon I-Y, Baek J-B (2012) Stability of multi-walled carbon nanotubes in commonly used acidic media. Carbon 50(4):1465–1476

[20] Rosca ID, Watari F, Uo M, Akasaka T (2005) Oxidation of multiwalled carbon nanotubes by nitric acid. Carbon 43(15):3124–3131

[21] Pimenta M, Dresselhaus G, Dresselhaus MS, Cancado L, Jorio A, Saito R (2007) Studying disorder in graphite-based systems by Raman spectroscopy. Phys Chem Chem Phys 9(11):1276–1290

[22] Moonoosawmy KR, Kruse P (2009) Ambiguity in the characterization of chemically modified single-walled carbon nanotubes: a Raman and ultraviolet–visible–near-infrared study. J Phys Chem C 113(13):5133–5140

[23] Osswald S, Flahaut E, Ye H, Gogotsi Y (2005) Elimination of D-band in Raman spectra of double-wall carbon nanotubes by oxidation. Chem Phys Lett 402(4):422–427

[24] Roy S, Das T, Yue CY, Hu X (2013) Improved polymer encapsulation on multiwalled carbon nanotubes by selective plasma induced controlled polymer grafting. ACS Appl Mater Interfaces 6(1):664–670

[25] Tang X-Z, Cao Z, Zhang H-B, Liu J, Yu Z-Z (2011) Growth of silver nanocrystals on graphene by simultaneous reduction of graphene oxide and silver ions with a rapid and efficient one-step approach. Chem Commun 47(11):3084–3086

[26] Tang X-Z, Li X, Cao Z, Yang J, Wang H, Pu X, Yu Z-Z (2013) Synthesis of graphene decorated with silver nanoparticles by simultaneous reduction of graphene oxide and silver ions with glucose. Carbon 59:93–99

[27] Compton OC, Dikin DA, Putz KW, Brinson LC, Nguyen ST (2010) Electrically conductive "alkylated" graphene paper via chemical reduction of amine-functionalized graphene oxide paper. Adv Mater 22(8):892–896

[28] Luo Z, Lim S, Tian Z, Shang J, Lai L, MacDonald B, Fu C, Shen Z, Yu T, Lin J (2011) Pyridinic N doped graphene: synthesis, electronic structure, and electrocatalytic property. J Mater Chem 21(22):8038–8044

[29] Zhang L, Ji L, Glans P-A, Zhang Y, Zhu J, Guo J (2012) Electronic structure and chemical bonding of a graphene oxide–sulfur nanocomposite for use in superior performance lithium–sulfur cells. Phys Chem Chem Phys 14(39): 13670–13675

[30] Biniak S, Szymański G, Siedlewski J, Światkowski A (1997) The characterization of activated carbons with oxygen and nitrogen surface groups. Carbon 35(12):1799–1810

[31] Haubner K, Murawski J, Olk P, Eng LM, Ziegler C, Adolphi B, Jaehne E (2010) The route to functional graphene oxide. ChemPhysChem 11(10):2131–2139

[32] Roy S, Das T, Ming Y, Chen X, Yue CY, Hu X (2014) Specific functionalization and polymer grafting on multi-walled carbon nanotubes to fabricate advanced nylon 12 composites. J Mater Chem A 2(11):3961–3970

[33] Lee H-J, Oh S-J, Choi J-Y, Kim JW, Han J, Tan L-S, Baek J-B (2005) In situ synthesis of poly (ethylene terephthalate)(PET) in ethylene glycol containing terephthalic acid and functionalized multiwalled carbon nanotubes (MWNTs) as an approach to MWNT/PET nanocomposites. Chem Mater 17(20):5057–5064

[34] Kwon O-S, Kim H, Ko H, Lee J, Lee B, Jung C-H, Choi J-H, Shin K (2013) Fabrication and characterization of inkjet-printed carbon nanotube electrode patterns on paper. Carbon 58:116–127

[35] Kordás K, Mustonen T, Tóth G, Jantunen H, Lajunen M, Soldano C, Talapatra S, Kar S, Vajtai R, Ajayan PM (2006) Inkjet printing of electrically conductive patterns of carbon nanotubes. Small 2(8–9):1021–1025

[36] Singh M, Haverinen HM, Dhagat P, Jabbour GE (2010) Inkjet printing—process and its applications. Adv Mater 22(6):673–685